Physicochemical characterization of D-mannitol polymorphs: The challenging surface energy determination by inverse gas chromatography in the infinite dilution region

María Graciela Cares Pacheco, Guadalupe Vaca Medina, Rachel Calvet, Fabienne Espitalier, Jean-jacques Letourneau, A. Rouilly, Élisabeth Rodier

Physicochemical characterization of D-mannitol polymorphs: The challenging surface energy determination by inverse gas chromatography in the infinite dilution region

M.G. Cares-Pacheco [a,*], G. Vaca-Medina [b,c], R. Calvet [a], F. Espitalier [a], J.–J. Letourneau [a], A. Rouilly [b,c], E. Rodier [a]

[a] Université de Toulouse, Mines Albi, UMR CNRS 5302, Centre RAPSODEE, Campus Jarlard, Albi cedex 09 F-81013, France
[b] Université de Toulouse, INP-ENSIACET, LCA, Toulouse 310130, France
[c] INRA, UMR 1010 CAI, Toulouse 310130, France

A B S T R A C T

Nowadays, it is well known that surface interactions play a preponderant role in mechanical operations, which are fundamental in pharmaceutical processing and formulation. Nevertheless, it is difficult to correlate surface behaviour in processes to physical properties measurement. Indeed, most pharmaceutical solids have multiple surface energies because of varying forms, crystal faces and impurities contents or physical defects, among others.

In this paper, D-mannitol polymorphs (α, β and δ) were studied through different characterization techniques highlighting bulk and surface behaviour differences. Due to the low adsorption behaviour of β and δ polymorphs, special emphasis has been paid to surface energy analysis by inverse gas chromatography, IGC. Surface energy behaviour has been studied in Henry's domain showing that, for some organic solids, the classical IGC infinite dilution zone is never reached. IGC studies highlighted, without precedent in literature, dispersive surface energy differences between α and β mannitol, with a most energetically active α form with a γ_s^d of 74.9 mJ·m^{-2}. Surface heterogeneity studies showed a highly heterogeneous α mannitol with a more homogeneous β (40.0 mJ.m^{-2}) and δ mannitol (40.3 mJ·m^{-2}). Moreover, these last two forms behaved similarly considering surface energy at different probe concentrations.

Keywords:
D-Mannitol
Crystallization
Polymorphism
Solid-state analytical techniques
Surface energy
Inverse gas chromatography

1. Introduction

Active pharmaceutical ingredients, APIs, must comply with well-defined specifications in terms of bioavailability, stability, toxicity, purity, morphology, stability, size, etc. Most of these substances can exist in several solid-state forms: polymorphs, pseudo-polymorphs, solvates/hydrates or amorphous forms depending on the generation, growth and formulation conditions. This diversity of solid forms requires a thorough understanding of solid-state phenomena that may occur in pharmaceutical engineering. Each of these forms has a different crystalline structure, and hence, different physicochemical properties. In the pharmaceutical field, the consequences related to polymorphism, habitus, surface state and particle size distribution does not relate only to APIs but also to excipients. Moreover, excipients play a key role in manufacturability but also in API's dissolution and bioavailability. Solid surface properties such as size, shape and powder agglomeration are also known to impact dissolution behaviour, compactability, aerosol performance and surface energetics among others (Ho et al., 2012; Tang et al., 2009).

Thus, to ensure a high quality to these organic solids, it is essential characterizing the solid-state forms, both in qualitative and quantitative ways. Characterization can be approached by a wide variety of analytical techniques. Over the last decade, the most frequently used solid-state techniques have been in decreasing order, X-ray powder diffraction (XRPD), differential scanning calorimetry (DSC), infrared spectroscopy (IR) and microscopy (Chieng et al., 2011). Most authors use at least two characterization techniques; however, all these methods give information at different levels or different depths within the solid and not especially on the surface. These days, it is well known that surface interactions play a fundamental role in mechanical operations such as grinding, milling and compaction, processes

* Corresponding author. Tel.: +33 5 63 49 32 26; fax: +33 5 63 49 30 25.
E-mail address: gcares@mines-albi.fr (M.G. Cares-Pacheco).

Nomenclature

$\mathcal{A}$(m^2)	Surface area of solid in contact with the adsorbed phase
A_{ads} (J)	Helmholtz free energy of the adsorbed phase
a_g(m^2/molecule)	Area occupied by an adsorbed probe molecule
a_s (m^2/g)	Specific surface area of the solid
F_{ads} (J)	Free energy of the adsorbed phase
F_s (cm^{3}STP/min)	Carrier gas flowrate at the exit of the column at 273.15–K and standard pressure
ΔG_{ads} (J)	Gibbs free energy variation for isothermal adsorption of n_{ads} moles of probe from n_g moles in gas phase initially
Δg_{ads} (J/mol)	Molar free energy variation for an isothermal adsorption of probe molecules
Δg_{CH_2} (J/mol)	Molar free energy variation for an isothermal adsorption of a methylene group
j (−)	James–Martin correction factor
K (m)	Henry's constant
m (g)	Sample mass
n_{ads} (mole)	Adsorbed mole number
N_a (molecules/mol)	Avogadro number
n_g (moles)	Number of gas moles
n_m (moles)	Monolayer capacity or number of adsorbed moles corresponding to a monolayer
n_{sol} (moles)	Solid mole number
P (Pa)	Vapour pressure
P_2 (Pa)	Vapour pressure of a pure component in equilibrium with its adsorbed phase at a spreading pressure π_2
R	Perfect gas law constant, 8314 J K^{-1} mol^{-1}
S_{ads} (J/K)	Entropy of the adsorbed phase
T (K)	Temperature
T_c (K)	Column temperature
t_N (min)	Net retention time
t_0 (min)	Dead time
t_R (min)	Retention time
V_{ads} (m^3)	Volume of the adsorbed phase
V_N (cm^3/g)	Net retention volume
W_{adh}(J/m^2)	Work of adhesion when adsorption occurs

Greek symbols

γ_c (J/m^2 or N/m)	Critical surface energy of a solid (used in Zisman theory)
γ_l^d (J/m^2 or N/m)	Liquid surface energy (or surface tension)
γ_s^d(J/m^2 or N/m)	Dispersive component of solid surface energy
γ_s (J/m^2 or N/m)	Total surface energy of a solid
γ_s^p (J/m^2 or N/m)	Polar component of solid surface energy
$\gamma_{CH_2}^d$ (J/m^2 or N/m)	Dispersive component of surface energy of a methylene group
θ (°)	C angle of a liquid on a solid
θ_s (−)	Surface coverage
μ_{ads}(J/mol)	Chemical potential of the adsorbed phase
μ_g (J/mol)	Chemical potential of the gas phase
π (J/m^2)	Spreading pressure of the adsorbate per unit surface area of solid
π_2 (J/m^2)	Spreading pressure of the adsorbate in equilibrium with its vapour phase at P_2
φ (J/mol)	Change in internal energy per mole unit of adsorbent due to the spreading of adsorbate

commonly used in pharmaceutical formulations but also in storage stability. Indeed, an important physicochemical property of solids is the surface energy because it reflects interfacial interactions between the solid and its environment. It seems, therefore, of utmost importance to examine and quantify the surface properties of a solid.

Organic solids are definitely complex systems. The complexity is related to the anisotropic nature of crystalline solids. In fact, it has been demonstrated that each face of a crystal or defects present in the solid structure has different surface properties generally attributed to different proportions of the functional groups exposed on it (Heng et al., 2006; Ho et al., 2010). Thus, a single value that represents the surface energy of a powder may be at best, a mean value.

A quite large number of methods have been used in the literature to determine surface energy on pharmaceuticals solids; contact angle, vapour adsorption techniques and atomic force microscopy (AFM). The most common methods are those that relate, directly or indirectly, surface energy to the contact angle formed between a liquid and a solid: spreading, capillary rise, Wilhelmy plate and heat of immersion. The limitations of these methods have been well reviewed but, even if the surface energy values obtained from contact angle measurements are somewhat inaccurate, the mean values obtained have been successfully correlated to functionality or end-use properties (Buckton, 1995; Buckton and Gill, 2007).

Nowadays, the study of the anisotropic surface properties of a solid goes through the investigation of solid–vapour interactions. In fact, wettability measurements are based on the interaction between a liquid and a solid surface. This leads to a macroscopic average of the surface energy, which is sensitive to surface roughness, porosity, packing structure and tortuosity of the porous material. On the contrary, gas–solid interactions give access to microscopic variations of the surface structure. Indeed, the study of the interactions between isolated gas molecules and the solid of interest will be sensitive to local variations of the surface at a molecular scale. Different characterization techniques are implemented based on vapour adsorption–desorption onto/from a solid, which are aimed to give information on specific surface area, porous structure and distribution (Rouquerol et al., 1999). The mechanisms of surface coverage and/or pore filling can be described by the study of a sorption isotherm. Indeed, the overall shape of the isotherm is governed by the gas–solid interactions, the solid's pore structure and temperature. A sorption isotherm relates the adsorbed vapour amount to the vapour concentration surrounding the solid in equilibrium conditions. Different parameters can be measured to determine an adsorption isotherm: the vapour pressure, the sample mass and the retention time. Each of these properties gives rise to a class of analytical techniques; manometric, gravimetric or chromatographic. However, very few are exploited to give surface energetic information; for that purpose, the two main techniques commonly used are dynamic vapour sorption (DVS) (Storey and Ymén, 2011) and inverse gas chromatography (IGC) (Ho and Heng, 2013; Mohammadi-Jam and Waters, 2014).

Object of a wide number of publications over the last decade, IGC appears to be a powerful technique to characterize the surface properties of divided solids (Ho and Heng, 2013). In general, chromatography is a separation technique based on the affinity between two phases, stationary and mobile one. Developed in the latest 50s, IGC is based on the physical adsorption of gas molecules on a solid surface. Unlike analytical gas chromatography (GC), where a known stationary phase is used to separate and identify an unknown mixture, in IGC the studied solid is the stationary phase, and well identified vapour molecules, called probes, are used to determine the interaction capacities of the unknown material packed into the column. The probe retention is the result of surface interactions between these gas molecules and the solid (Conder and Young, 1977). These physical interactions are dominated by van der Waals forces, whose magnitude depends on the probe nature for a fixed solid, allowing then both chemical and morphological studies of divided solids. In addition, IGC allows to study the influence on solid surface of factors such as humidity (Buckton and Gill, 2007), physical (Heng et al., 2006) and/or chemical treatments (Ho et al., 2010).

As we already noticed, it is well known that solids are anisotropic systems. Literature devoted to the surface heterogeneity assessment from adsorption measurements is exhaustively reviewed in the works of Jaroniec and Madey (1988) and Rudzinski and Everett (1992). To represent the existence of a distribution of energy sites on a solid surface exploiting IGC data, the energy distribution function, $\chi(\in)$, is generally used.

This physical model supposes an energetically heterogeneous surface with a continuous distribution of adsorption energies, which can be described as a sum of homogeneous adsorption patches. This approach has been well reviewed by Balard (1997) who has focused his work on the study of inorganic solids (Balard et al., 2008; Papirer et al., 1991, 1999; Boudriche et al., 2011). Another way to study surface heterogeneity has been proposed by Fafard et al. (1994) using IGC in infinite dilution conditions; this will be described next.

The first applications of IGC in the field of pharmaceuticals began in the latest 80s. The first approach was focused on the determination of Hansen solubility parameters of lactose, caffeine, theophylline and methyl hydroxybenzoate (Phuoc et al., 1987, 1986). It had not been until 1994 that the technique was used for the surface energy characterization of pharmaceutical solids. The studies conducted by (Ticehurst et al., 1994) on salbutamol sulphate and α-lactose put in evidence the sensitivity of the technique to detect small differences in crystallinity between batches, differences undetected by other techniques such as DSC (Ticehurst et al., 1996). Nowadays, polymorphism remains a challenging issue for IGC, maybe due to the upstream difficulty obtaining the different pure crystalline forms of a pharmaceutical solid and/or because of the instability of the polymorphic system during analysis. In spite of such difficulties, amorphous pharmaceuticals, which are of great interest because of their better solubility, and thus, better bioavailability, have been the subject of several studies (Brum and Burnett, 2011; Miyanishi et al., 2013; Surana et al., 2003).

Mannitol has been chosen for the current study, in particular because of the kinetic and thermodynamic stability of its polymorphic system. D-Mannitol, or (2R–5R)-hexane-1,2,3,4,5,6-hexol according to IUPAC nomenclature, is a polyhydric alcohol with the chemical formula $C_6H_{14}O_6$. It is one of the most common excipients in pharmaceutical products due to its chemical stability and non-hygroscopicity. As an active ingredient, it has been used for treating renal failure and intracranial hypertension and more recently as a bronchoconstrictor (Tang et al., 2009). Several publications in relation to D-mannitol polymorphs can be found; however, they are somewhat confusing and sometimes even contradictory. D-Mannitol can exist as four crystalline forms, three anhydrous forms namely α, β and δ and a hemihydrate one. The δ form is enantiotropically related to α and β forms. The most stable form is β-mannitol, and the less stable at ambient conditions is the δ form. Nevertheless, it has been observed that the unstable form, δ, can be stable for a period of at least 5 years at room temperature, if stored in dry environment (Burger et al., 2000).

Both physicochemical properties and polymorphic transformation between crystalline forms of D-mannitol that may occur in crystallization, mechanical milling and thermal treatment studies have been successfully characterized by multiple solid-state analytical methods (Bruni et al., 2009; Burger et al., 2000; Caron et al., 2007). Surface energy analyses by IGC have highlighted the acidic nature of the β form, attributed to the high density of hydroxyl groups at mannitol surface (Saxena et al., 2007). In addition, IGC has been used to differentiate two optical forms of mannitol, the racemic mixture DL and D-mannitol composed of only one stereoisomer in its anhydrous β. Grimsey et al. (1999) found that the dispersive interactions were stronger for the racemic mixture DL-mannitol. Using molecular modelling, the authors attributed this different behaviour to the different densities of the dispersive and acidic sites. More recently, investigations concerning D-mannitol have been focused on the effect of milling or/and surface heterogeneity (Ho et al., 2010, 2012). Despite its widespread use in pharmaceutical formulations, studies on the surface energetic properties of mannitol polymorphs have been rarely reported.

The current study focuses on the surface energetics of D-mannitol polymorphs through dynamic contact angle measurements, DVS and IGC implementation. Finally, the solid anisotropy is studied to evaluate surface heterogeneity at low surface coverage. The dual aim of this work is to highlight the differences between surface and bulk properties of anhydrous forms of D-mannitol and to compare the surface energy determination techniques used for pointing out their relevance considering the physical sense of the measure.

2. Polymorphs generation and characterization

2.1. Polymorphs generation

2.1.1. Materials

Analytical grade organic solvents, acetone and methanol (MeOH), were purchased from Fluka and Across Organic respectively, both with a mass fraction purity higher than 99.5%. High purity deionized water (18 MΩ) was obtained from a laboratory purification system.

D-Mannitol and sorbitol were generously supplied by Roquette. The batch, Pearlitol 160C, is composed of 99% of β mannitol mass percentage and only 1% of sorbitol. The batch, Pearlitol 200SD, is composed of a mixture of β and α mannitol while the batch Neosorb P100T is composed of sorbitol but no information about polymorphic composition has been given. The solubility of D-mannitol was determined for each dissolution medium. Due to the high sensitivity of the HPLC Hi-Plex column to organic solvents, the solubility values were determined by two different ways. HPLC was used only when the solvent was pure water, and classic solvent evaporation (dry extract method) was implemented when solvent was water/acetone or methanol. The solubility of the commercial batch Pearlitol 160C in water was found to be 157 mg per g of solution at 20 °C. For the mixture water/acetone with a volume ratio of 1:1, the solubility at 20 °C was found to be 34 mg per g of solution. For pure methanol at 60 °C, the solubility was found to be 5 mg per g of solution. It has to be noted that the dry extract method is less precise than the HPLC quantification method,

because it does not allow to quantify sorbitol influence, but it was the only one feasible.

2.1.2. Protocols

The recrystallization of pure β and δ polymorphs was obtained through crystallization of an aqueous solution of D-mannitol using acetone as an antisolvent according to the following steps:

- Dissolution of 9 g of D-mannitol in 50 g of water under stirring at room temperature for at least 2 h.
- Filtration of the suspension using a Büchner filter equipped with a 2 μm polyethylene membrane.
- Addition of 50 ml of acetone at room temperature, maintaining a vigorous stirring.

To obtain the δ form, the crystals were allowed to grow for maximum 4 min. For the β form, longer time periods were used, allowing the polymorphic transformation.

For the α mannitol generation, a crystallization procedure by seeding and fast cooling was used according to:

- Dissolution of D-mannitol in methanol at 60 °C for 2 h under stirring (2 g in 250 ml of MeOH).
- Filtration of the suspension using a Büchner filter equipped with a 2 μm polyethylene membrane.
- Seeding with a pure physical α form obtained by DSC, as follow:

  - *First cycle*: heating rate of 20 °C min^{-1} from 20 to 200 °C followed by a cooling cycle with a rate of 5 °C min^{-1} until 20 °C.
  - *Second cycle*: heating rate of 20 °C min^{-1} from 20 to 160 °C followed by a cooling cycle with a rate of 5 °C min^{-1} until 20 °C.

- Fast cooling of the filtrate in an ice–ethanol bath under vigorous stirring for 30 min.

For all samples, the same filtration, drying and storage conditions were used, that is a Büchner filtration with a 2 μm polyethylene membrane followed by a drying in an oven under vacuum, at 30 °C and 200 mbar for at least 3 days. Finally, all solid samples were stored in a dessiccator under vacuum (6% relative humidity). In order to remove the sorbitol impurity from the commercial powder, at least two consecutive recrystallization processes have been performed per organic solid.

2.2. Characterization techniques

The different crystalline forms of anhydrous mannitol α, β and δ were characterized by HPLC to quantify chemical impurities and by solid-state analytical methods such as DSC, XRPD, TGA, SEM, IR, confocal Raman spectroscopy, DVS and IGC to quantify and qualify physical properties.

2.2.1. Polymorphs finger prints

X-ray diffractograms were obtained using a PANanalytical X'Pert Pro MPD diffractometer (set-up Bragg–Brentano). Diffraction data are acquired by exposing the powders samples to Cu-Kα radiation, which has a wavelength of 1.5418 Å. The generator was set to 45 kV and to a current of 40 mA. The data were collected over a range of 8–50° 2θ with a step size of 0.03° 2θ and a nominal time per step of 39.9 s, using the scanning X'Celerator detector. Data analysis was performed using X'Pert Data Collector software and phase identification was carried out by means of PANalytical High Score Plus software in conjunction with the ICDD Powder Diffraction File 2 database and the Crystallography Open Database.

Raman spectroscopy analyses were performed with an atomic force microscope equipped with a confocal Raman imaging upgrade, Alpha 300 from WITec. The positioning accuracy of the scan table is 1.5 nm in *XY* direction and 0.3 nm in *Z* direction. A magnification of 50× and a wavelength of 532 nm was used as the excitation source, Nd:YAG laser. The Raman data were acquired using WITec Project Plus software that has a 16 bits resolution and a sampling rate of 250 Hz.

Infrared spectra were collected on a Thermo Scientific Nicolet 5700 FT-IR spectrometer equipped with an attenuated total reflection module (ATR).

DSC measurements were performed with a DSC Q200 from TA Instrument. Measurements were performed on samples of 3–5 mg placed in non-hermetic aluminium panels, in the temperature range of 20–200 °C at a heating rate of 5 °C min^{-1}. All data measurements are averages of at least three measures on three different samples. Thermogravimetric analyses were performed using an TGA-DSC 111 from Setaram on samples of 5–20 mg placed in non-hermetic aluminium panels, performing cycles from 25 to 250 °C at a heating rate of 5 °C min^{-1}.

2.2.2. Size and particle shape analysis

Particle shape analyses were performed by scanning electron microscopy, using a XL30 FEG from Philips. Particle size analyses for the anhydrous forms of D-mannitol were determined by image analysis using a PharmaVision System 830 (PVS 830) from Malvern Instruments. The particles dispersion pressure was set at 6 bar. The number of analysed objects was fixed at 70,000.

2.3. Characterization results, polymorphs screening

2.3.1. Powder crystallinity and purity

The chemical purity of each polymorph was checked by HPLC using a Hi-Plex Ca ligand exchange column coupled with a refractive index detector (analysis conditions: mobile phase HPLC grade water, flow rate 0.3 ml min^{-1}, column temperature 45 °C).

XR diffractograms of D-mannitol pure forms are shown in Fig. 1 and the IR spectra in Fig. 2. Both results are in agreement with those published in the literature (Burger et al., 2000), even if no information on chemical purity was given. Despite the fact that each technique provides meaningful information, and no sample preparation is required, both techniques may not be sensitive enough and have their own limitations. Indeed, no significant differences between the commercial powder (1% of α-sorbitol) and the recrystallized β form were detected. Anyway, detection of small quantities is complex and may depend on the location of sorbitol within the powder, near to (at) the surface or within the bulk of the crystals.

The Raman spectra of D-mannitol polymorphs are shown in Fig. 3. These are in excellent agreement with those published in the

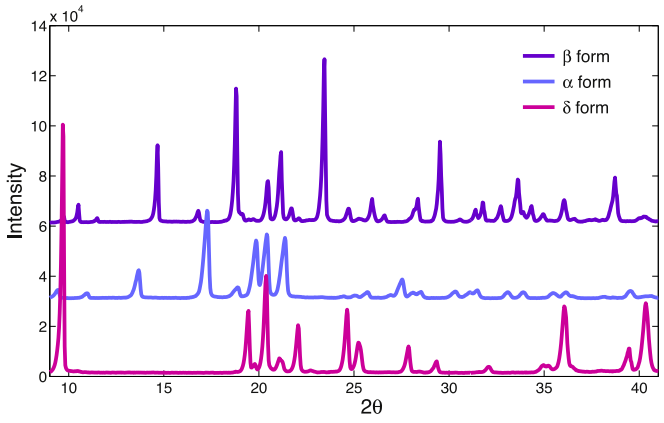

Fig. 1. X-ray diffractograms of D-mannitol polymorphs.

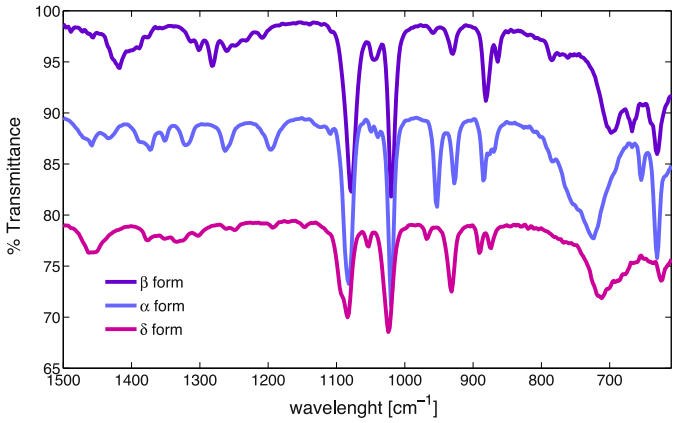

Fig. 2. IR spectra of D-mannitol polymorphs.

literature (Burger et al., 2000; Hao et al., 2010). Confocal Raman spectroscopy seems to be a sensitive characterization technique, and it has been used to study polymorph mixtures. Nevertheless, no qualitative or quantitative analysis of the sorbitol presence in the commercial powder has been relevant, maybe due to the fact that D-mannitol and its isomer, sorbitol, differ only by the stereochemistry of one hydroxyl group (inducing subtle intra- and inter-molecular behaviour differences) or due to the low sample mass used in the analysis (some micrograms). Finally, the chemical purity of the samples was confirmed by thermal methods.

Thermogravimetric analyses by TGA were used to ensure that no residual solvent was present in the samples. DSC analyses allowed differentiating the commercial powder Pearlitol 160C from the β pure form. Indeed, sorbitol presence in the commercial powder decreases both heat of fusion and melting point of β polymorph. The first endothermic peak at 81.4 °C, found during the analysis of the commercial powder, is consistent with the melting point of α sorbitol (Nezzal et al., 2009). The endothermic/exothermic event observed in δ form was attributed to a transformation of this crystalline form into a more stable β form. Close values of melting points between α and β mannitol indicate small volume energetic differences. All these results presented in Table 1 are in agreement with those found in the literature (Bruni et al., 2009; Burger et al., 2000).

For the determinations of the heat of fusion, using a sigmoid baseline, a standard deviation of less than 5% was estimated while melting points values are more accurate with a standard deviation of less than 0.5% (six measures average).

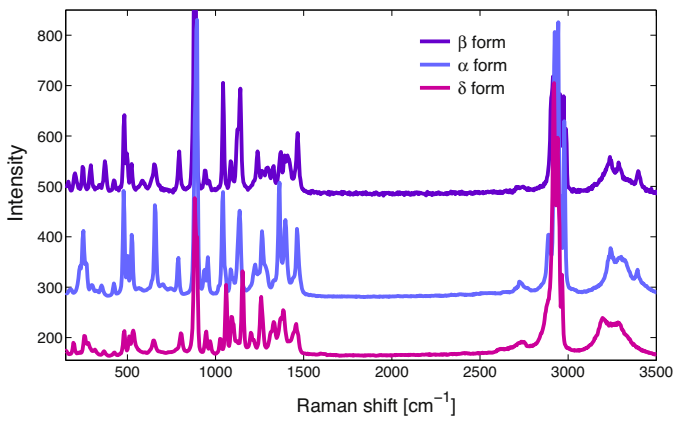

Fig. 3. Raman spectra of D-mannitol polymorphs.

2.3.2. Particle size and morphology

As shown in Figs. 4 and 5, the morphology of each polymorph and the commercial samples is different. Important differences can be also found in the literature, mostly attributed to the differences in recrystallization procedures (Bruni et al., 2009; Ho et al., 2012). As expected, since β and δ mannitol are generated by the same method, both forms are alike with thinner sticks for δ mannitol. Size differences are linked to crystal growth duration. The α form is the finest one with a needle-shape morphology and a $D[v, 0.5]$ of 25.3 μm and $D[v, 0.9]$ of 42.4 μm (Fig. 4b). The commercial sample Pearlitol 160C is formed by irregular sticks with a median volume diameter $D[v, 0.5]$ of 64 μm and a $D[v, 0.9]$ of 250 μm (Fig. 5a). β Mannitol is composed of better defined sticks with smoother surfaces (Fig. 4a), and it has a $D[v, 0.5]$ of 26.7 μm and a $D[v, 0.9]$ of 81.7 μm. In both cases, it seems that small particles get stuck on the surface of larger ones.

3. Surface behaviour

The surface energy of a solid, γ_s, can be defined as the half of the energy of cohesion, which is the energy required to separate and then create two interfaces of unit of surface area from a primarily monolithic material and further displace one separated part to infinity (in adiabatic, reversible conditions) (Lee, 1991). This energy of cohesion is also the energy of interaction between molecules and atoms under consideration. The surface energy can be approached through the interactions of the solid with its environment, and then through the nature of the intermolecular forces involved in the physisorption process. Indeed, surface energy can be divided into dispersive, γ_s^d, and non-dispersive components, γ_s^p. The study of non-polar molecules as *n*-alkanes will give access to γ_s^d value while the study of molecules with permanent dipole moments, electrical charges, which may give rise to acid–base, ionic or metallic interactions among others, will give access to γ_s^p values.

Whatever the system probe–solid, dispersive interactions always occur, they are the focus of the present work.

3.1. Theoretical basis

This study is limited to the most widespread techniques and specific attention will be paid to the isotherm section exploitation. Gravimetric adsorption techniques such as DVS (dynamic vapor sorption) are based on the gravimetric measurement of the amount of vapour adsorbed on the surface of a solid. This technique allows to determine a mean value of the surface energy of a powder based on the whole isotherm information (Storey and Ymén, 2011). Indeed, during DVS analysis a complete surface coverage can be reached.

While wettability and DVS measurements provide a macroscopic average of the surface, techniques such as inverse gas chromatography, IGC, can be sensitive to local microscopic variations of the surface structure depending on the injection size. In practice, IGC experiments are generally performed according to two implementations, which differ by the amount of probe molecules injected. The first implementation, called infinite dilution, IGC-ID, is defined by the injection of very small quantities of molecules. Experimentally, is expected that the retention time or volume remains constant in function of the injection size; thus, probe molecules behaves independently (condition of linear chromatography). The second one, called finite concentration, IGC-FC, is based on higher solute concentrations (non-linear chromatography), and some degree of

Table 1
Summary of physical solid-state characterization obtained by DSC.

	Pearlitol 160C	Neosorb P100 T	Pearlitol 200SD	β-Form	α-Form	δ-Form
Heat of fusion [J g^{-1}]	300.20.4	179.7	292.10.2	304.5	294.4	0.9/−2.1 Melting/recrystallization
Melting point [°C] (onset)	165.6 81.4	96.8	165.1 68.6	166.7	165.3	146.8/156.2 Melting/recrystallization

interaction between probe molecules is expected (Conder and Young, 1977).

However, while studying D-mannitol polymorphs that are low specific surface area organic solids, some concerns and questions had arisen to actually differentiate these two domains of implementation: at which relative pressure, P/P_{sat}, range is the IGC-ID zone limited? How small should be the injection size to actually obtain retention times independent of the gas molecules concentration? Moreover, is the linear part of the adsorption isotherm defined by symmetric or slightly asymmetrical chromatograms as admitted in literature?

To try to answer these questions, surface energy values were estimated exploiting only the linear part of the adsorption isotherm at very low surface coverage. This will be presented next but, above all, preliminary bases of IGC theory need to be presented. In particular, thermodynamic approach of physisorption on a solid surface is reminded so as to point out the specificities of solid-adsorbed vapour system underlying the classical results used when interpreting IGC results.

3.1.1. Basic IGC theory

The time spent for a probe molecule to pass through the column, t_R, reflects the interactions between the vapour molecules and the solid; it is then the key measure in IGC analysis. The strength of these interactions depends on the solid nature and structure (surface heterogeneities), the nature and quantity of the probe molecules.

As shown in Fig. 6, a fraction of this residence time, called dead time, t_0, corresponds only to the time for a probe molecule to flow through the solid without any interaction and can be determined by a non-adsorbed molecule such as methane. Then, net retention time is defined as:

$$t_N = t_R - t_0 \tag{1}$$

Taking into account the pressure drop along the column using the James–Martin correction factor, j, it is possible to relate t_N to the net retention volume per sample mass unit, V_N, through:

$$V_N = \frac{j}{m} F_s t_N \frac{T_c}{273.15} \tag{2}$$

where m is the solid mass, F_s is the carrier gas exit flow rate at standard temperature and pressure, and T_c is the column temperature.

Relating a retention time or volume, to a surface energy value needs to introduce some additional concepts. First of all, it is assumed that the solid on which adsorption occurs, adsorbent, remains unchanged in structure and is chemically inert. The probe molecules in the adsorbed state called adsorbate may be regarded as a distinct phase whose volume is considered negligible compared to the probe molecules in the vapour phase, also called adsorptive. The diminution of the surface tension, due to physisorption, is called the spreading pressure, π, and is the intensive variable that characterizes the adsorbed phase. According to Ruthven approach (Ruthven, 1984), a new free energy thermodynamic function can be defined as:

$$F_{ads} = A_{ads} + \varphi n_{sol} \tag{3}$$

where n_{sol} is the mole number of adsorbent while φ represents the change in internal energy per mole unit of adsorbent due to the spreading of the adsorbate over the adsorbent surface, A_{ads} is the Helmholtz free energy of the system adsorbate–adsorbent.

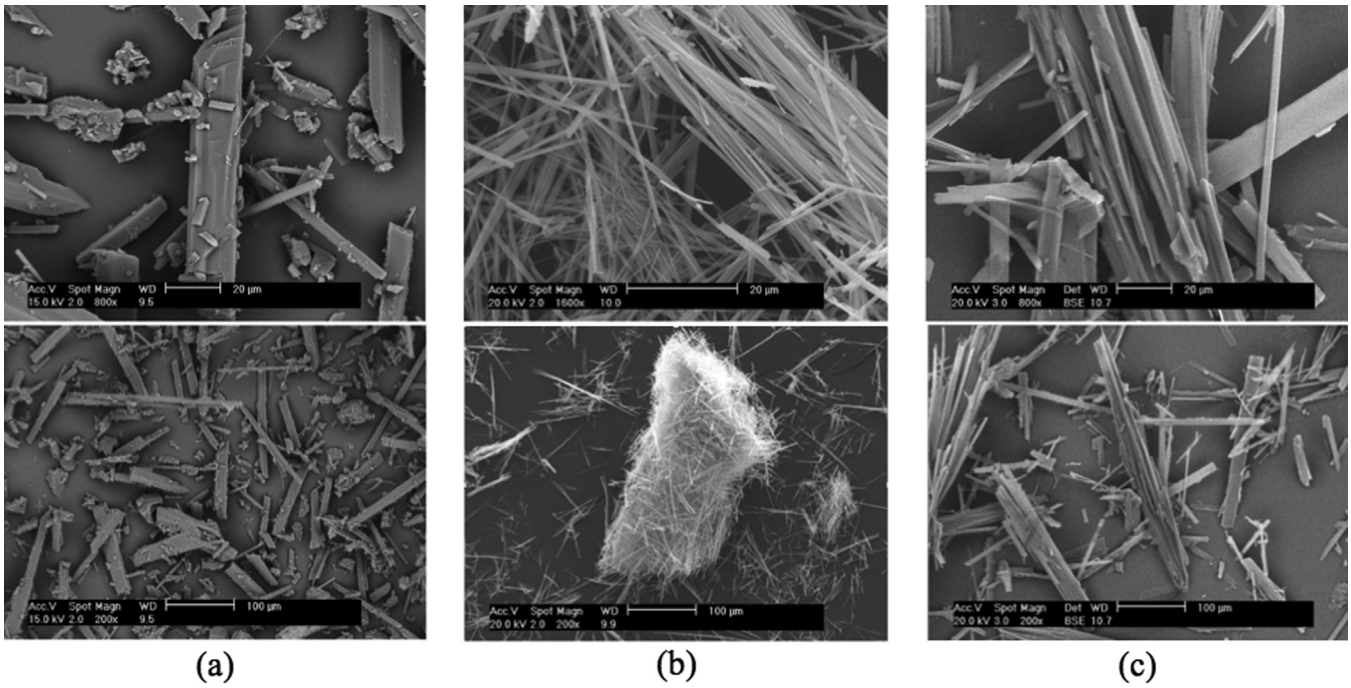

Fig. 4. SEM micrographs of D-mannitol polymorphs; (a) β form, (b) $\propto$ form and (c) δ form.

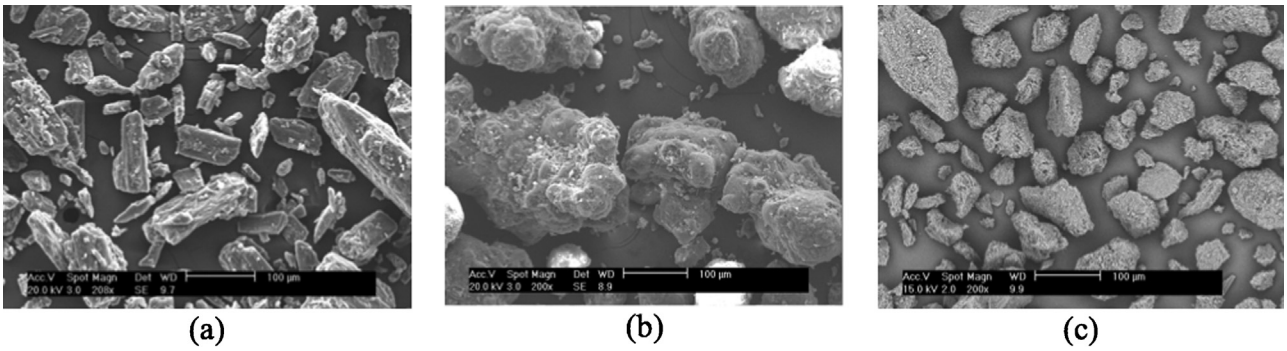

Fig. 5. SEM micrographs of commercial powders; (a) Pearlitol 160C, (b) Pearlitol 200SD and (c) Neosorb P100T.

For adsorption on a two-dimensional surface, the surface area $\mathcal{A}$ in contact with the adsorbed molecules is directly proportional to n_{sol}. So the product φn_{sol} is equivalent to $\pi\mathcal{A}$. Hence, Eq. (3) turns into:

$$F_{ads} = A_{ads} + \pi\mathcal{A} \tag{4}$$

In case of gas adsorption, the gas transfer will occur lowering the free energy of the system until equilibrium is reached (F_{ads} is minimum). The equilibrium of the adsorbate is represented by the following fundamental thermodynamic equation, which combines the first and second laws:

$$dF_{ads} = -S_{ads}dT - PdV_{ads} + Ad\pi - \mu_{ads}dn_{ads} \tag{5}$$

Thanks to the Euler's homogeneous function theorem, F_{ads} can also be integrated as:

$$F_{ads} = -PV_{ads} + \mu_{ads}n_{ads} \tag{6}$$

Subtracting Eq. (5) to the differential of the function six leads to an equilibrium relation like the Gibbs–Duhem one:

$$-S_{ads}dT - V_{ads}dP + \mathcal{A}d\pi - n_{ads}d\mu_{ads} = 0 \tag{7}$$

Given that the adsorbed phase volume is generally negligible, the relation that links variables along an isothermal adsorption is then:

$$\mathcal{A}\left(\frac{\partial\pi}{\partial P}\right)_T - n_{ads}\left(\frac{\partial\mu_{ads}}{\partial P}\right)_T = 0 \tag{8}$$

Equilibrium conditions between the adsorbed phase and the adsorptive one imply the equality of their chemical potentials. In addition, adsorptive phase is assumed to behave as an ideal gas. In this case, Eq. (8) leads to the Gibbs adsorption isotherm:

$$\mathcal{A}\left(\frac{\partial\pi}{\partial P}\right)_T = n_{ads}\left(\frac{\partial\mu_g}{\partial P}\right)_T = \frac{RT}{P}n_{ads} \tag{9}$$

Depending on the probe molecules concentration, the adsorbed phase may obey to different equations of state. At very low concentrations, it is supposed to obey an equation of state equivalent to ideal gas law according to:

$$\pi\mathcal{A} = n_{ads}RT \tag{10}$$

In this case, the Gibbs adsorption isotherm becomes:

$$\left(\frac{\partial\pi}{\partial P}\right)_T = \frac{\pi}{P} \tag{11}$$

Integration of Eq. (11) leads to the Henry's law, that is a linear relation between adsorptive pressure and adsorbate spreading pressure through a constant K:

$$K = \frac{\pi}{P} \text{ or } \frac{n_{ads}}{A} = K\frac{P}{RT} \tag{12}$$

We consider now the isothermal adsorption of n_{ads} moles of adsorbate at a spreading pressure π_2 in equilibrium with $n_g - n_{ads}$ moles of gas phase at a pressure P_2 from a gaseous phase comprising initially n_g moles at a pressure P_1. The variation of free enthalpy of adsorption can be expressed as:

$$\Delta G_{ads} = n_{ads}\mu_{ads}(T,\pi_2) + (n_g - n_{ads})\mu_g(T,P_2) - n_g\mu_g(T,P_1) \tag{13}$$

where π_2 is the equilibrium spreading pressure at P_2, both being related by $K = \pi_2/P_2$.

Final conditions of this adsorption are equilibrium ones. The chemical potential of the adsorbed phase can then be expressed as that adsorptive ideal gas one. Eq. (13) turns into:

$$\Delta g_{ads} = \frac{\Delta G_{ads}}{n_g} = RT\ln\frac{P_2}{P_1} = -RT\ln\frac{P_1K}{\pi_2} \tag{14}$$

As it was already enlightened, the measured value that gives access to the equilibrium conditions is the retention volume V_N, and it can be directly related to the equilibrium constant K from Eq. (12):

$$V_N = \frac{n_{ads}RT}{P} = KA = Ka_sm \tag{15}$$

Taking into account, all the hypotheses previously described and relating Eqs. (14) and (15), the volume V_N can be related to the change in molar free energy of adsorption by:

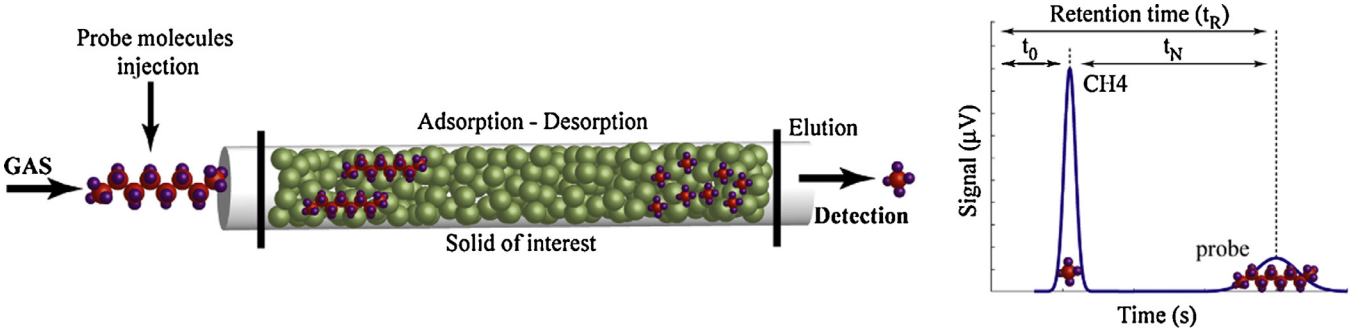

Fig. 6. Principle of inverse gas chromatography.

$$\Delta g_{ads} = -\mathrm{RTln}\frac{P_1 V_N}{\pi_2 a_s m} \quad (16)$$

Experimentally, T is taken to be the column temperature, T_c.

The first approach to quantify surface energy overcoming the unknown arbitrary values, π_2 and P_1 dilemma, was suggested by Dorris and Gray in 1979. Their model is based on the observation that in a chemical family of homologues, the retention time is an exponential function of the number of carbon atoms (Derminot, 1981). Experimentally, it is necessary to inject a series of n-alkanes and plot the variation of the term $-RT\ln V_N$ versus the number of carbon atoms. The slope of this line is the variation of the free energy of the system during the adsorption of a methylene group, Δg_{CH_2};

$$\Delta g_{CH_2} = -\mathrm{RTln}\frac{V_{N+1}}{V_N} \quad (17)$$

In addition, the change in free energy of adsorption can be understood as the adhesion of two phases due to the interaction forces between them and described by the energy of interaction or its opposite, the work of adhesion (that is the work necessary to overcome the interactions forces). If the probe molecules are n-alkanes and the adsorption takes place on a non-polar solid, the interaction forces are dominated by dispersive interactions (London type). Applying the model of Fowkes for Lifshitz-van der Waals interactions representing the work of adhesion, W_{adh}, the Gibbs free energy of adsorption, Δg_{ads}, can be expressed as follows:

$$\Delta g_{ads} = N_a a_g W_{adh} = N_a a_g 2\sqrt{\gamma_l^d \gamma_s^d} \quad (18)$$

Finally Eqs. (17) and (18) leads to:

$$\Delta g_{CH_2} = N_a a_{CH_2} 2\sqrt{\gamma_{CH_2}^d \gamma_s^d} = -\mathrm{RTln}\frac{V_{N+1}}{V_N} \quad (19)$$

where a_{CH_2} is the surface area, $6 \times 10^{-18}\,m^2$, and $\gamma_{CH_2}^d$ is the surface energy of a methylene group, ($35.6\,mJ\,m^{-2}$ at 20 °C).

3.1.2. Surface energy profile

The SEA analysis software, Cirrus Plus from SMS company, proposes to study surface heterogeneity using IGC-ID basis, and it is the one used in this research work. Surface heterogeneity studies using IGC-ID basis have been proposed by Fafard et al. (1994) and described by Ylä-Mäihäniemi et al. (2008). As can be depicted from Fig. 7, the γ_s^d profile is determined by injecting a series of alkanes at different concentrations.

The aim is to relate different probe molecules concentrations to a surface coverage of these molecules over the solid, to finally correlate the surface coverage to a surface energy value.

In our case, first order method (FM) was used to study adsorption isotherms from IGC elution chromatograms. In the FM method as in the peak maximum method (PM), different concentrations of probe molecules (corresponding to different P/P_{sat}) are injected into the column (Fig. 7 – step 1).

The net retention volume, V_N, can be determined for each injection concentration using the net retention time obtained from first order moment (Eq. (2)) of the elution peak. To relate V_N to surface coverage, n/n_m, the software calculates the desorbed amount, n, from peak area analysis. Since monolayer capacity, n_m, for each alkane is calculated from the BET adsorption model, surface coverage can be calculated from the desorbed amount, n, at each probe concentration (Fig. 7 – step 2). As illustrated in Fig. 7, for each alkane at a particular surface coverage γ_s^d can be calculated classically using IGC-ID theory via Dorris–Gray and/or Schultz approaches. Finally, each γ_s^d value can be related to a surface coverage value (Fig. 7 – step 4).

3.2. Surface analyses techniques

3.2.1. Materials

Analytical grade organic solvents such as ethanol, toluene, dichloromethane, diiodomethane, formamide, ethylene glycol 33% and 1,4-dioxane were purchased from Fluka or Across Organic all of them with a mass fraction purity higher than 99.5%. The non-polar probes octane, nonane, decane and undecane were purchased from Sigma, assay >99%.

3.2.2. Protocols

Dynamic contact angles were obtained with a Krüss processor tensiometer K12 in combination with a K software. The powder samples were placed in a stainless steel holder with holes in its bottom small enough to avoid the powder flowing through them. The samples, previously packed with a centrifuge at 1000 rpm during 5 min, were suspended from the microbalance placed in the processor tensiometer just above the surface of the test liquid. The liquid reservoir was kept at 20 °C (293 K) with a thermostated bath (Haak K20/DC5).

Gas adsorption manometry was performed in an ASAP 2010 instrument from Micromeritics. Each sample was degassed under vacuum at 50 °C (323 K) during at least 72 h. For comparison purpose, argon was used as the adsorption gas. The analyses were carried out at a temperature of −196 °C (77 K) (liquid nitrogen).

Gas adsorption analyses by gravimetry were carried out in a dynamic vapour sorption (DVS-2) instrument from surface measurement systems SMS. The DVS measures sample mass evolution using a Cahn microbalance with a resolution

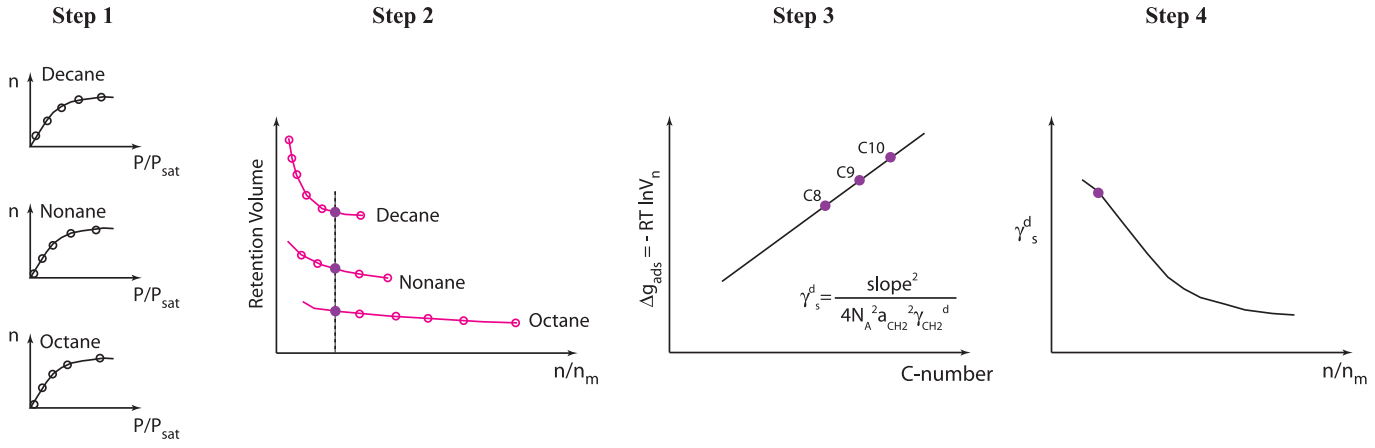

Fig. 7. Determination of surface energy profile by IGC-SEA.

experimentally determined at 5 μg. During the analyses, a vapour flow constituted of a mixture of probe-saturated and dry carrier gas (nitrogen) surrounds the sample. The partial pressure of the probe is controlled using mass flow controllers, and the whole system is kept isothermal by an enclosed cabinet fixed at 25.0 °C (297 K). Isotherms were measured using analytical grade *n*-nonane as non-polar probe and different polar probes such as isopropanol and ethanol were also tested. The sample size was typically 70 mg, and at least one cycle of adsorption–desorption was studied: a cycle consists of mass measurements versus time until equilibrium is reached, performed at fixed increasing (decreasing) values of partial pressure vapour probe (P/P_{sat}). The sorption isotherms values calculated are then, the equilibrium mass values obtained at each partial pressure with an equilibrium criterion of mass variation lower than 5 μg during 5 min.

Specific surface area and surface energy analyses of D-mannitol polymorphs were carried out using the IGC-surface energy analyser (IGC-SEA) from SMS. Each polymorph sample was packed into pre-silanised columns of 300 mm length and 4 mm internal diameter, plugged with silanised glass wool. Prior to analysis, each column was conditioned at 50 °C for 2 h at 0% RH. Helium was used as a carrier gas at 10 sccm, and the column temperature was fixed at 30 °C (303 K) during the analysis, all experiences were undertaken in identical conditions. Due to the progressive spreading of the probe molecules with the migration time, the adsorption isotherms and the net retention volume, V_N, were determined using peak center of mass, which corresponds to the FM method (Giddings, 1965). The retention times of probe molecules and methane were determined using a flame ionization detector (FID). Dead volume was determined by methane injections and dispersive surface energy determination by a homologous series of vapour *n*-alkanes (undecane, decane, nonane and octane). Dispersive surface energy profiles were calculated using Cirrus Plus software (version 1.2.3.2 SMS, London) following Dorris–Gray and Schultz approaches.

For all specific surface area and surface energy determinations, a standard deviation of less than 5% was estimated. For comparison purposes, all columns were filled with a mass of powder corresponding to a surface area of 0.5 m^2. The idea was to study similar surface coverage values obtained experimentally.

Unlike others IGC equipments, IGC-SEA has an injection device that allows to control the injection size, and so it works fixing specific surface coverage values. The corresponding surface coverage, θ_s, at each injection concentration is the ratio between the desorbed amount, *n*, determined from peak area and the monolayer capacity of the solid, n_m ($\theta_s = n/n_m$). In our experiments, n_m was determined from the specific surface area value obtained by IGC-SEA using *n*-nonane as probe molecule.

3.3. Results and discussion

3.3.1. Surface energetics characterization by wetting force: capillary penetration method

The first approach to determine surface energy was through dynamic contact angle studies. The aim was on one hand, to evaluate the wettability of mannitol using different liquids, allowing us to determine which solvents should be used for DVS analyses, on the other hand to test the surface energy estimation by this approach. To undertake this, two commercial batches were used. In fact, this type of analysis involves high quantities of powder, so the batch Pearlitol 160C was used to evaluated β mannitol, and the batch Pearlitol 200SD was used to evaluate α mannitol behaviour. Contact angle measurements on bulk powders using the capillary penetration are presented in Table 2. The geometric factor *C*, linked to packing characteristics, was determined using *n*-hexane, and the error associated to all the measures was evaluated as the standard deviation of four measurements.

Table 2
Dynamic contact angle measurements on D-mannitol commercial powders by capillary rise.

Solvant	Contact angle θ [°]	
	Pearlitol 160C $C = 3.4 \times 10^{-5}$ [cm^5]	Pearlitol 200SD $C = 1.75 \times 10^{-5}$ [cm^5]
n-Hexane	0.0	0.0
n-Octane	38.0 ± 4.0	–
n-Nonane	38.6 ± 3.2	0.0
Ethanol	43.1 ± 4.1	26.1 ± 2.5
Toluene	41.5 ± 2.8	0.0
Dichloromethane	43.1 ± 4.1	21.0 ± 2.0
1,4-Dioxane	47.3 ± 1.6	0.0
Diiodomethane	76.4 ± 0.7	55.7 ± 2.3
Formamide	–	58.5 ± 2.6
Ethylene glycol 33%	84.2 ± 1.5	75.6 ± 1.7
Water	79.1 ± 0.3	61.3 ± 3.4

Several theories can be used to convert contact angle data into surface energy values. The objective is to find a proper combination of test solvents knowing that the surface energy value depends on the liquids that are used and the theory that is chosen. The surface energy results obtained by capillary rise, using Owens–Wendt and Fowkes models, are gathered in Table 3.

The model proposed by Owens, Wendt, Rabel and Kaelble defines surface energy as a sum of a dispersive component and a polar component (Owens and Wendt, 1969). The surface energy values were evaluated without using water and ethanol as solvents for improving the fit confidence ($R^2_{160C} = 0.956$ and $R^2_{200SD} = 0.909$). For water, it seems that the hydrophilic character of mannitol does not ensure that the mechanism of liquid uptake is only adsorption, and a partial dissolution of the powder could occur. Fowkes model has similar basis as the model above but determines the two components, dispersive and non-dispersive, taking into account the spreading pressure, π (Fowkes, 1964). In contact angle measurements, Fowkes model is generally applied only with two liquids, water and diiodomethane. In our case, we used diiodomethane to evaluated dispersive interactions and ethylene glycol 33% rather than water to evaluated polar interactions.

Contact angle analysis allows to choose the solvents needed for DVS studies highlighting the difficulties of solvent choice for β mannitol analysis, for which acceptable wettability behaviour ($\theta \rightarrow 0$) is limited to *n*-hexane. For α mannitol, *n*-nonane was used as probe molecule to study γ_s^d and polar molecules as dichloromethane and ethanol, to study γ_s^p component.

As a conclusion, capillary rise measurements give a global approach of the solid surface energy, being aware of the limitations and the relativity of the accuracy (low R^2 results) of the values gathered in Table 2, we have shown consistency between Owens–Wendt and Fowkes models.

3.3.2. Surface energetics characterization by adsorption techniques: solid–vapour interactions

All the results obtained from solid–vapour adsorption techniques are gathered in Table 4. Specific surface area values were determined by three different techniques such as manometry

Table 3
Surface energy [mJ m^{-2}] analysis determined by capillary rise and different models approach.

Solid/model	Owens and Wendt			Fowkes		
	γ_s^d	γ_s^p	γ_s	γ_s^d	γ_s^p	γ_s
Pearlitol 160C	18.7	4.8	23.5	19.5	4.7	24.2
Pearlitol 200SD	27.6	6.1	33.7	31.1	4.2	35.3

Table 4
Specific surface areas and dispersive surface energies of D-mannitol polymorphs.

Solids	Specific surface area a_s $[m^2 \cdot g^{-1}]$			Dispersive surface energy γ_s^d $[mJ \cdot m^{-2}]$			
	ASAP-Ar	DVS	IGC-C_9	DVS	CGI $\theta_s = 0.04\%$	CGI $\theta_s = 0.6\%$	CGI $\theta_s = 8\%$
Pearlitol 160C	0.41	–	0.37	–	70.7	61.6	44.9
Pearlitol 200SD	1.59	C_7-0.9	1.68	49.5	81.1	80.2	54.9
Neosorb P100T	1.16	–	4.40	–	45.4	45.1	42.4
β-Form	0.39	–	0.37	–	40.0	39.6	38.2
α-Form	8.40	C_9-5.61	8.54	51.4	74.9	74.0	45.5
δ-Form	–	–	1.01	–	40.3	40.4	38.4

using argon (ASAP), gravimetry using DVS and IGC with alkanes as probe molecules for both last ones. All data exploitation is based on the BET adsorption model.

For the DVS analysis, the baseline instrument stability was especially important due to the fact that the absolute levels of vapour uptake were in the detection limits at low P/P_{sat}. In fact, the absolute vapour uptakes were low, typically less than 0.3%. As an example for the commercial form, Pearlitol 160C, an adsorption of 0.025% at P/P_{sat} close to one was obtained, while for β and δ-mannitol a mass uptake smaller than 0.3% was obtained at the same pressure ratio.

To study surface energy from a gravimetric technique such as DVS, the surface tension of the solvent has to be taken into account to have accurate values (*n*-hexane $\gamma_s^d = 18.4\,mJ\,m^{-2}$ and *n*-nonane $\gamma_s^d = 22.7\,mJ\,m^{-2}$). Indeed, the probe molecules must have a surface tension lower than the solid surface energy (i.e. liquid must wet the surface solid, $\theta \rightarrow 0^\circ$). Also, the vapour uptake must be adsorption and thermodynamic equilibrium at all partial pressures must be reached. So, as expected from dynamic contact angle results (Table 2), DVS studies have been successfully performed for the batch 200SD and the pure α form. Moreover, despite the physical composition differences, the obtained isotherms showed a classic type II BET shape revelling similar adsorption behaviour ($\sim 50\,mJ\,m^{-2}$).

For all IGC experiences, an experimental value of t_N for each probe molecule, at each surface coverage value, was fundamental in order to avoid any meaningless extrapolation. Thus, due to the limitations of SEA injection system, *n*-heptane was not used as probe molecule because it cannot be injected at low surface coverage values ($\theta_s < 0.01$). Concerning *n*-undecane, it cannot be injected at $\theta_s > 0.01$, but, even if it can be injected at really low $\theta_s \sim 0.0001$, noisy signals were obtained, and problems of return to the baseline after injection were observed. Also, for *n*-undecane, strong differences between peak maximum and peak center of mass were found, showing important asymmetry of the outlet pulse peaks, which induced a great error in the R^2 values obtained for the alkanes line (step 3 on Fig. 7). Thus, to study surface energy of D-mannitol polymorphs, C_8, C_9 and C_{10} were used as probe molecules. Nevertheless, for C_8, a linear approximation was used to obtain low surface coverage values since it cannot be injected at $\theta_s < 0.001$.

In case of polar interactions studies, all vapour probes could not be injected at low surface coverage values ($\theta_s < 0.02$), and asymmetrical chromatograms were obtained. As it was not possible to determine Henry's region, only *n*-alkanes are the focus of this work.

In IGC-ID, a very low concentration of vapour probe is injected. Thus, no probe-probe molecular interactions are expected to occur and the adsorption follows Henry's law. The chromatograms have a Gaussian shape, and the retention time is independent of the amount of probe injected. For some organic solids, this region may be difficult to observe, the specific surface area and the intensity of the interactions seem to play a key role. Indeed, in the case of low surface area samples, the monolayer capacity of the solid is easily reached ($\theta_s = 1$). Thereby, a precise control of the injected amount is crucial to study surface energy at the "zero concentration region".

Most authors define the IGC-ID zone at low vapour concentrations, typically for $P/P_{sat} < 0.03$. To verify this statement for organic solids, in our experiments, the Henry region was defined for each probe molecule. The chosen criterion was linearity of the adsorption isotherm, with a correlation coefficient $R^2 > 0.999$. For almost all solids studied, the so defined Henry's region revealed to be composed of two zones. The first one was characterized by chromatograms having a Gaussian shape and by the fact that the retention time was independent of the amount of probe molecules injected, as shown in Fig. 8a. This IGC-ID region was found to be limited to really low surface coverage values: for β, δ mannitol and

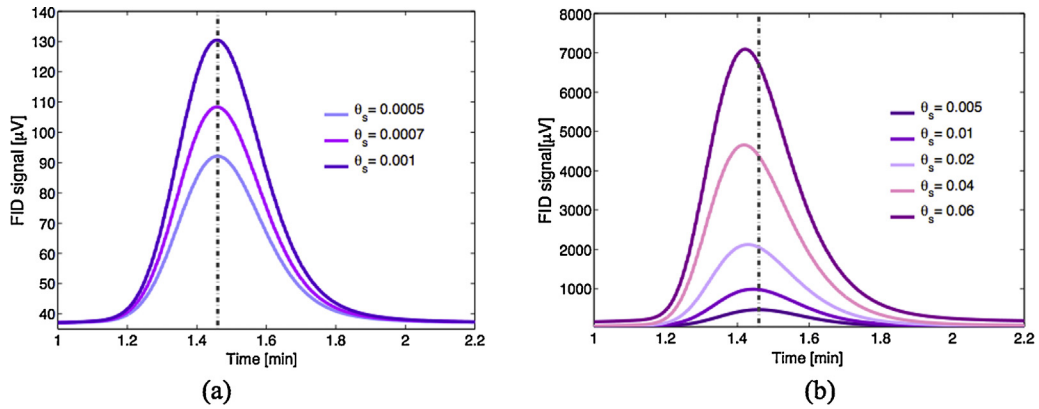

Fig. 8. Chromatograms of D-mannitol at different surface coverage, using *n*-nonane as probe molecule, within Henry's region.

Pearlitol 160C, this zone was limited to $\theta_s < 0.001$. The second zone was characterized by a decrease of the net retention time with increasing surface coverage (Fig. 8b). For α, mannitol t_N was never independent of the injected amount, so the first zone was never reached. This difference can be attributed to high solid surface heterogeneity (Fig. 9) and to the strength of the interactions involved.

As shown in Table 4, the α form is the most energetically active form with γ_s^d of 74.9 mJ m^{-2} at $\theta_s = 0.04\%$. These founding highlight the potential of pure α polymorph in dry powder inhaler (DPI) formulations. Nowadays, it is well known that surface properties play a fundamental role in the drug-carrier interaction. Tang et al. (2009) studied surface energy of different D-mannitol batches to explain aerosol performance. The authors concluded that higher surface energy powders can lead to an improvement of the respirable fraction of the active ingredient. It has to be noted that surface energy analysis must to be performed together with particles dynamics studies (packing, contact area and detachment). Indeed, particles shape is an important factor in aerosol performance. It seems that needle-like particles reach easier deep lungs deposition with optimum therapeutic benefit (Tang et al., 2009). The higher surface energy batch obtained by the authors is composed of a mixture of α and β mannitol. From our results, this high value is attributed to the presence of α form, which generates more cohesive and adhesive powders. Indeed, the presence of α mannitol in the commercial powder 200SD seems to highly influence the mixture behaviour (Table 4).

The most commonly used carrier is α lactose monohydrate with a γ_s^d of ~40 mJ m^{-2} at P/P_{sat} ~0.04 (Heng et al., 2006). Nevertheless, it has been shown that lactose can promote chemical degradation of some active pharmaceutical ingredients when used in formulations as an excipient (Guenette et al., 2009). Thus, α mannitol having a high surface energy, stability and well defined needle-shape morphology is a possible candidate for use as a bronchoconstrictor in DPI formulations.

The stable β form is less active with γ_s^d of 40.0 mJ m^{-2} and not much different of δ form with γ_s^d of 40.3 mJ m^{-2}. After DVS analysis, where vapour uptake levels were in the detection limits range, doubts about isotherm type (II or III) have arisen for these two forms. Unfortunately, the adsorption behaviour cannot be studied at $\theta_s > 1$ with IGC-SEA equipment to confirm (disconfirm) isotherm type. Besides, significant differences have been found between the commercial powder and the β pure form obtained by crystallization. These differences could be mostly attributed to particles morphology; the recrystallized β mannitol seems to be more "homogeneous" (Fig. 4a) than the commercial powder (Fig. 5a). Anisotropies in the morphology of the commercial form can be seen as high energetic sites that influence the surface energy value obtained at low surface coverage.

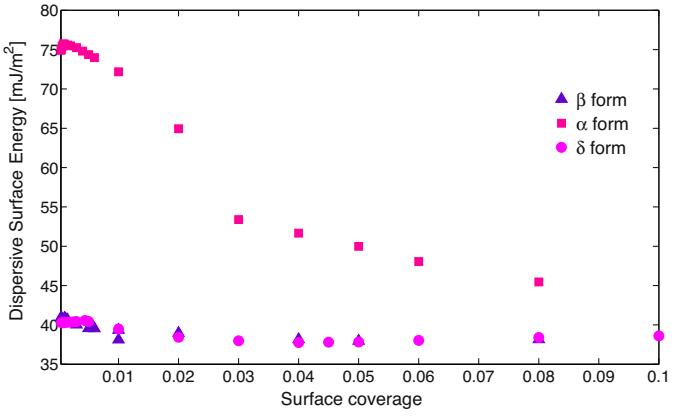

Fig. 9. Surface heterogeneity analysis of D-mannitol polymorphs using Dorris ang Gray model.

Sorbitol influence on β mannitol, through Pearlitol 160C batch, was not quantified. Indeed, sorbitol surface behaviour was evaluated via the commercial batch Neosorb P100T. Nevertheless, DSC analysis highlighted that this batch is constituted mostly of γ-sorbitol (45 mJ m^{-2}) while the polymorphic form present in the batch Pearlitol 160C may most likely be α-sorbitol, which is a metastable form not available pure commercially (Nezzal et al., 2009).

The surface energy value obtained for the stable β form is in agreement, but lower, with those obtained in the literature via contact angle on a single macroscopic crystal using Owens–Wendt model (Ho et al., 2010). Indeed, crystalline β mannitol obtained in this research is closer to the less energetically active facet (0 1 1) than to the more energetically active one (0 1 0) determined by the authors (44.0 mJ m^{-2}). Saxena et al. (2007) studied surface energy by dynamic molecular modelling and determined a γ_s^d of 56.2 mJ m^{-2} for the plan (0 2 0) and a γ_s^d of 55.3 mJ m^{-2} for the plan (1 1 0). Nevertheless, these high values were never obtained in this research work.

The results obtained via IGC at $\theta_s = 3\%$ for the commercial powder Pearlitol 160C are similar to those obtained by Ho et al. (2010) with a γ_s^d of 49.5 mJ m^{-2}. Moreover, these values are also similar to those obtained by Saxena et al. (2007) using IGC-ID classical approach (P/P_{sat} ~0.03), with a γ_s^d of 48.2 mJ m^{-2}.

Dorris–Gray and Schultz models have been used to determine γ_s^d. Nevertheless, Schultz model showed slightly lower R^2 values for almost all polymorphs at almost all surface coverage values. These results are in agreement with the results of Ylä-Mäihäniemi et al. (2008). The authors attributed this fact to the uncertainty of the cross-sectional area of molecules involved in Schultz equation (influence of molecular shape and temperature). Nevertheless, these differences were not that critical in this work.

The surface energetics profiles obtained using Dorris–Gray approach are shown in Fig. 9. A criterion of the fit $R^2 > 0.999$ for the line formed by the alkanes was used to ensure the quality of the data (Fig 7 – step 3). This restriction correlates quite well with the Henry's zone determined by isotherms analysis, but it was not exclusive. Indeed, it was found that for some solids this criterion could be checked for larger surface coverage values, which were not related to isotherm linearity. As an example, in case of β mannitol, Henry's domain is limited to $\theta_s < 10\%$ while a fit of $R^2 > 0.999$ were obtained for $\theta_s < 40\%$.

It seems important to highlight the difficulties to determine Henry's domain. Indeed, for solids with high surface interactions, as α mannitol, isotherm shape can be quite well described at $\theta_s < 30\%$. For solids with low surface interaction, as β and δ mannitol, a high precision and control of the injected amount is fundamental to determine linearity domain; so is an adequate number of experimental points.

As it can be noted from Fig. 9, β and δ forms seem to be more energetically homogeneous than the α form. Moreover non-significant differences between β and δ have been found. These results can be in agreement with the statements of Ho et al. (2012), where the authors propose that the surface energy distribution does not depend on total surface area of the sample but is dependent on the contribution of energetic sites present on the solid.

Differences obtained between DVS and IGC-ID analyses for α mannitol are attributed to the physical sense of each surface energy determination. The DVS result represents the average of all energetics sites present in the solid. Indeed, in DVS analyses a complete coverage of the solid surface was reached and so an average value of the surface energetics is expected. Contrariwise, in IGC-ID studies the dispersive surface energy is generally attributed

to the higher energetic sites of the surface. If the studied solid is homogeneous, energetically speaking, both techniques are comparable. When the surface heterogeneity is studied (Fig. 9) using IGC-ID theory in the Henry's domain, we can see that the surface energetics of α mannitol goes from 75.7 to 45.5 mJ m^{-2}. This last value is closer but lower than the results obtained by DVS, 51.4 ± 2.9 mN m^{-1}. These results are difficult to explain because IGC analyses were made at really low surface coverage, $\theta_s < 12\%$, showing a highly heterogeneous surface, for which energetics profile is more influenced by the higher energy sites. Indeed, retention time distribution can be described as:

$$t_N = \sum n_i \tau_i = \sum_i n_i \tau_0 e^{E_i/RT_c}$$

with τ_i the residence time on the site i,E_i interaction energy between the probe and the site i, and τ_0 a constant.

Thus, IGC values should never be smaller than those obtained by DVS. To get more conclusive surface analysis, heterogeneity should be studied by IGC-FC using the adsorption energy distribution model (Balard, 1997) or/and by contact angle in a macroscopic crystal.

From a critical point of view, the injection system of the IGC-SEA equipment allows to control the injected amount of vapour molecules, and moreover, allows to inject small quantities of it. These assets have been extremely important in this work because they were the key to determine Henry's domain in low specific surface area solids. However, there are some points that cannot be neglected while using the SEA equipment to determine surface energy. The first one is that the surface coverage ratio defined by SMS, n/n_m, is a mean value based on the hypothesis that molecules are equally distributed over the surface solid. This does not reflect reality because of the nature of the chromatographic elution process (Giddings, 1965).

The second one is that the Dorris–Gray or Schultz approaches have to be applied in the Henry's law region where lateral molecular interactions are negligible, and the thermodynamics functions depend only on adsorbate–adsorbent interactions (for isotherms type II, IV and V). Hence, the determination of Henry's region of the adsorption isotherm should be performed with care, experimental data points should be numerous enough (Fig. 7 – step 1). Another point that should be taken into account is that these methods are also based on surface homogeneity assumption, so only one energy site is expected. Assuming that solids are heterogeneous and that the variation of the net retention time in Henry's region is due to a multi-sites surface, it seems necessary to notice that the γ_s^d value attributed to each surface coverage does not correspond to an average energy value of the sites "visited" by the probes molecules and is specific to a given surface coverage. Careful interpretation of these numerical values has to be made.

4. Conclusions

The results obtained enlightened significant differences between bulk and surface properties of D-mannitol polymorphic system. As each technique provides specific information of the solid, the combination of these techniques allows a good understanding of the solid-state form. The combined set DSC and IGC solid-state techniques highlight both surface-bulk energetic differences. Moreover, DSC solid-state analyses were found to be a reliable technique to determine both polymorph physical purity and sorbitol detection within the samples.

Surface energy analysis through dynamic contact angle studies gives a global idea of solids wettability and so helps to define solvents of interest for studies by DVS and IGC. Nevertheless, surface energy values obtained for the commercial powders by dynamic contact angle were substantially lower than those obtained by DVS and IGC. These differences can be attributed to the lower fit confidence values, $R^2 < 0.96$, obtained for all models studied Owens–Wendt and Fowkes.

DVS analysis was non exploitable for most of the studied solids. In fact, due to the low adsorption at low pressures, β and δ forms were in the detection limits, and it was not possible to analyses them. It seems that DVS analysis is not suitable for the analysis of solids with low specific surface area and weak adsorbent–adsorbate interactions (adsorption behaviour). Nevertheless, it gives a global view of the adsorption behaviour between probe molecule and the solid, allowing to determine isotherm type and to quantify the spreading pressure.

IGC studies highlighted, with no precedent in literature, surface energy differences between the forms α and β mannitol: α mannitol revealed to be more energetically active with a γ_s^d of 74.9 mJ m^{-2} ($\theta_s \rightarrow 0$) while β mannitol showed a value of 40.0 mJ m^{-2} ($\theta_s \rightarrow 0$) similar to δ mannitol (40.3 mJ m^{-2}). These results explain and corroborated the use of α polymorph as a dry powder inhaler (DPI), increased by its needle-shape morphology.

To study surface heterogeneity by IGC-ID basis, it seems fundamental to determine the zone where Henry's law holds, due to the fact that all thermodynamics assumptions are based on linear chromatography. Indeed, it seems that for low specific surface area solids this region is almost not observable, so for reliable surface energy estimation, a precise control of the injected amount is crucial in order to obtain very low surface coverage. It should to be noted that low specific surface area seems not to be the only restriction to the limited Henry's region; the interactions strength and surface heterogeneity seem to have a more significant impact.

The well-known infinite dilution, or linear chromatography, is defined by Henry's region. In case of D-mannitol, the word linear in the sense that the Henry's coefficient, K, is independent of the probe concentration was never obtained for the α form. In practice, the observed peaks are quite asymmetrical and dependent of the injection size (for both peak maxima and first order moment). Thus, in the whole sense of its definition, this so defined ID region reveals to be absent or almost non-observable.

Surface heterogeneity analysis, in Henry's domain, showed a highly heterogeneous α mannitol (74.9 to 45.5 mJ m^{-2}) with a quite homogeneous β and δ mannitol. Moreover, no significant differences between these last two forms have been detected (~40–38 mJ m^{-2}).

The influence of size and morphology in surface energy behaviour of D-mannitol polymorphs is the subject of separate paper currently in preparation.

Acknowledgments

The authors would like to acknowledge Sylvie del Confetto, Severine Patry and Veronique Nallet for technical support. Gratefully acknowledges to Roquette France for the provision of the pharmaceuticals solids used in this work.

References

Balard, H., Maafa, D., Santini, A., Donnet, J.B., 2008. Study by inverse gas chromatography of the surface properties of milled graphites. J. Chromatogr. A 1198–1199, 173–180.

Balard, H., 1997. Estimation of the surface energetic heterogeneity of a solid by inverse gas chromatography. Langmuir 13, 1260–1269.

Boudriche, L., Calvet, R., Hamdi, B., Balard, H., 2011. Effect of acid treatment on surface properties evolution of attapulgite clay: an applicationof inverse gas chromatography. Colloids Surf. A 392, 45–54.

Brum, J., Burnett, D., 2011. Quantification of surface amorphous content using dispersive surface energy: the concept of effective amorphous surface area. AAPS PharmSciTechnol. 12, 887–892.

Bruni, G., Berbenni, V., Milanese, C., Girella, A., Cofrancesco, P., Bellazzi, G., Marini, A., 2009. Physico-chemical characterization of anhydrous -mannitol. J. Therm. Anal. Calorim. 95, 871–876.
Buckton, G., Gill, H., 2007. The importance of surface energetics of powders for drug delivery and the establishment of inverse gas chromatography. Adv. Drug Delivery Rev. 59, 1474–1479.
Buckton, G., 1995. Interfacial Phenomena in Drug Delivery and Targeting. Harwood Academic.
Burger, A., Hetz, J., Rollinger, S., Weissnicht, J.M., 2000. Energy/temperature diagram and compression behavior of the polymorphs of -mannitol. Int. J. Pharm. Sci. 89, 457–468.
Caron, V., Willart, J.F., Danède, F., Descamps, M., 2007. The implication of the glass transition in the formation of trehalose/mannitol molecular alloys by ball milling. Solid State Commun. 144, 288–292.
Chieng, N., Rades, T., Aaltonen, J., 2011. An overview of recent studies on the analysis of pharmaceutical polymorphs. J. Pharm. Biomed. Anal. 55, 618–644.
Conder, J.R., Young, C.L., 1977. Physicochemical Mesuarements by Gas Chromatography. John Wiley, Chichester.
Derminot, J., 1981. Physicochimie des polymères et surface par chromatographie en phase gazeuse. Technique et documentation, Paris.
Dorris, G., Gray, D., 1979. Adsorption of n-alkanes at zero surface coverage on cellulose paper and wood fibers. J. Colloid Interface Sci. 77, 353––362.
Fafard, M., El-Kindi, M., Schreiber, H.P., Dipaola-Baranyid, G., Hore, A.M., 1994. Estimating surface energy variations of solids by inverse gas chromatography. J. Adhes. Sci. Technol. 8, 1383–1394.
Fowkes, F.M., 1964. Attractive forces at interfaces. Ind. Eng. Chem. 56, 40–52.
Giddings, C.J., 1965. Dynamic of Chromatography. Marcel Dekker Editor, London.
Grimsey, I.M., Sunkersett, M., Osborn, J.C., York, P., Rowe, R.C., 1999. Interpretation of the differences in the surface energetics of two optical forms of mannitol by inverse gas chromatography and molecular modelling. Int. J. Pharm. Sci. 191, 43–50.
Guenette, E., Barretta, A., Krausa, D., Brodya, R., Hardinga, L., Mageea, G., 2009. Understanding the effect of lactose particle size on the properties of DPI formulations using experimental design. Int. J. Pharm. 380, 80–88.
Hao, H., Su, W., Barret, M., Caron, V., Healy, A.M., Glenon, B., 2010. A calibration-free application of raman spectroscopy to the monitoring of mannitol crystallization and its polymorphic transformation. Org. Process Res. Dev. 14, 1209–1214.
Heng, J.Y., Thielmann, F., Williams, D., 2006. The effects of milling on the surface properties of form I paracetamol crystals. Pharm. Res. 8, 1918–1927.
Ho, R., Heng, R., 2013. A review of inverse gas chromatography and its development as a tool to characterize anisotropic surface properties of pharmaceutical solids. Kona Powder Part. J. 30, 164–178.
Ho, R., Hinder, S., Watts, J., Dilworth, S., Williams, D., Heng, J., 2010. Determination of surface heterogeneity of mannitol by sessile drop contact angle and finite concentration inverse gas chromatography. Int. J. Pharm. 387, 79–86.
Ho, R., Naderi, M., Heng, J., Williams, D., Thielmann, F., Bouza, P., Keith, A.R., Thiele, G., Burnett, D., 2012. Effect of milling on particle shape and surface heterogeneity of needle-shaped crystals. Pharm. Res. 29, 2806–2816.
Jaroniec, M., Madey, R., 1988. Physical Adsorption on Heterogeneous Solids, Studies in Physical and Theoretical Chemistry. Ed. Elsevier, Amsterdam, NL.
Lee, L.-H., 1991. Fundamental of Adhesion. Plenum Press, New York.
Miyanishi, H., Nemoto, T., Mizuno, M., Mimura, H., Kitamura, S., Iwao, Y., Noguchi, S., Itai, S., 2013. Evaluation of crystallization behavior on the surface of nifedipine solid dispersion powder using inverse gas chromatography. Pharm. Res. 30, 502–511.
Mohammadi-Jam, S., Waters, K.E., 2014. Inverse gas chromatography applications: a review. Adv. Colloid Interface Sci. doi:http://dx.doi.org/10.1016/j.cis.2014.07.002.
Nezzal, A., Aerts, L., Verspaille, M., Henderickx, G., Rendl, A., 2009. Polymorphism of sorbitol. J. Cryst. Growth 311, 3863–3870.
Owens, D.K., Wendt, R.C., 1969. Estimation of the surface free energy of polymers. J. Appl. Polym. Sci. 13, 1742–1747.
Papirer, E., Li, S., Balard, H., Jagiello, J., 1991. Surface-energy and adsorption energy-distribution measurements on some carbon-blacks. Carbon 29, 1135–1143.
Papirer, E., Brendle, E., Ozil, F., Balard, H., 1999. Comparison of the surface properties of graphite, carbon black and fullerene samples: measured by inverse gas chromatography. Carbon 37, 1265–1274.
Phuoc, N.H., Phan Tan Luu, R., Munafo, A., Ruelle, P., Nam-Tran, H., Buchmann, M., Kesselring, U.W., 1986. Determination of partial solubility of lactose by gas–solid chromatography. J. Pharm. Sci. 75, 68–72.
Phuoc, N.H., Phan Tan Luu, R., Munafo, A., Ruelle, P., Nam-Tran, H., Buchmann, M., Kesselring, U.W., 1987. Determination of partial and total cohesion parameters of caffeine, theophylline, and methyl *p*-hydroxybenzoate by gas–solid chromatography. J. Pharm. Sci. 76, 406–410.
Rouquerol, F., Rouquerol, J., Sing, K., 1999. Adsorption by Powders and Porous Solids; Principles, Methodology and Applications. Academic Press, London.
Rudzinski, W., Everett, D.H., 1992. Adsorption of Gases on Heterogeneous Surfaces. Ed. Academic Press Inc., San Diego, pp. 92101.
Ruthven, D.M., 1984. Principles of Adsorption and Adsorption Processes. John Wiley & Sons, New York.
Saxena, A., Kendrick, J., Grimsey, I., Mackint, L., 2007. Application of molecular modelling to determine the surface energy of mannitol. Int. J. Pharm. 343, 173–180.
Storey, R., Ymén, I., 2011. Solid State Characterization of Pharmaceuticals, first ed. Wiley, Kingdom United.
Surana, R., Randall, L., Pyne, A., Vemuri, M., Suryanarayanan, R., 2003. Determination of glass transition temperature and in situ study of plasticizing effect of water by inverse gas chromatography. Pharm. Res. 20, 1647–1654.
Tang, P., Chan, H., Chiou Ogawa, K., Jones, M.D., Adi, H., Buckton, G., 2009. Characterisation and aerosolisation of mannitol particles produced via confined liquid impinging jets. Int. J. Pharm. 367, 51–57.
Ticehurst, M.D., Rowe, R., York, P., 1994. Determination of the surface properties of two batches of salbutamol sulphate by inverse gas chromatography. Int. J. Pharm. 111, 241–249.
Ticehurst, M.D., York, P., Rowe, R.C., Dwivedi, S.K., 1996. Characterisation of the surface properties of a-lactose monohydrate with inverse gas chromatography, used to detect batch variation. Int. J. Pharm. 141, 93–99.
Ylä-Mäihäniemi, P., Heng, J., Thielmann, F., Williams, D., 2008. Inverse gas chromatographyc method for measuring the dispersive surface energy distribution for particulates. Langmuir 24, 9551–9557.